Journal of Materials Chemistry C

Accepted Manuscript

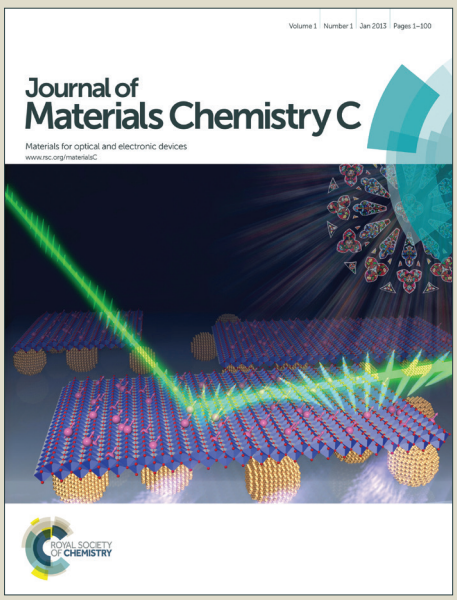

ROYAL SOCIETY OF CHEMISTRY

www.rsc.org/materialsC

Graphic Abstract for:

Mechanofluorochromic Behaviors of β-Iminoenolate Boron Complexes Functionalized with Carbazole

Noble β-iminoenolate boron complexes exhibit totally different mechanofluorechromic properties due to the excimer and monomer tranformation.

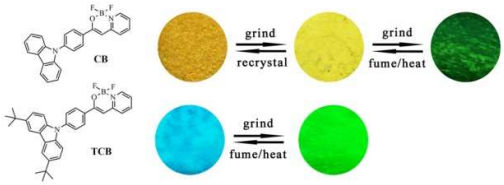

Journal Name

RSCPublishing

ARTICLE

Mechanofluorochromic Behaviors of β-Iminoenolate Boron Complexes Functionalized with Carbazole

Cite this: DOI: 10.1039/x0xx00000x

Zhenqi Zhang, [a] Pengchong Xue, [a,b] Peng Gong, [a] Gonghe Zhang, [a] Jiang Peng [a] and Ran Lu [a,*]

Received 00th January 2012,
Accepted 00th January 2012

DOI: 10.1039/x0xx00000x

www.rsc.org/

Carbazole and *tert*-butylcarbazole functionalized β-iminoenolate boron complexes **CB** and **TCB** with different mechanofluorochromic (MFC) properties have been synthesized. It was found that the as-synthesized crystal of **CB** emitted orange light under UV illumination because of the appearance of the emission from the monomers and the excimers. After grinding for a while, the ground powder 1 of **CB** emitted bright yellow light since the ratio of the emission intensity from excimers/monomers decreased. Further grinding for a long time, the excimers disappeared and the obtained amorphous ground powder 2 emitted dark green light. However, **TCB** emitted sky blue light in the as-synthesized crystal because no excimer was formed due to the steric hindrance of *tert*-butyl. After grinding, the amorphous ground powder of **TCB** emitted bright green light derived from excimer. It should be noted that the fluorescent quantum yield of **TCB** in amorphous solid state reached 0.53, which was the highest one for the β-iminoenolate boron complexes that have ever been reported. In addition, the emission changes of **CB** and **TCB** in different solid states were reversible upon repeating treatment of mechanic grinding and fuming with CH_2Cl_2. Therefore, the obtained β-iminoenolate boron complexes might be used as sensors and memory chips on the basis of the solid fluorescence response to external mechanical force and organic solvent.

Introduction

Organic solid-state luminescent materials have received much attention due to their potential applications in organic light-emitting diodes (OLEDs),[1] organic light-emitting field-effect transistors (OLEFETs),[2] organic solid-state lasers[3] and organic fluorescent sensors.[4] Much efforts have been made in designing π-conjugated compounds with strong solid emission. In general, the fluorescent emission properties of the dye molecules in dilute solutions can be easily predicted by means of quantum chemical calculations. However, the emission of the chromophores would often become complicated in solid states since the conformations of the molecules and the molecular packing modes in solid states would affect the solid emission. Recently, the mechanofluorochromic (MFC) emissive organic materials, whose emitting colors change in response to external mechanical forces (such as grinding, crushing, rubbing, etc.) and can be restored to the original states by annealing or fuming with organic vapors, have gained an increasing interest[5] because such kind of "smart" materials may be employed in luminescence switches,[6] mechanosensors,[7] data storage,[8] security inks,[9] and optoelectronic devices.[10] Till now, it has been found that the derivatives of tetraphenylethene,[11] 9,10-divinylanthracene[12] and oligo(*p*-phenylene vinylene)[13] exhibit MFC properties because of their loose molecular packing in crystals which can be damaged easily under external stimuli. For example, Löwe et al. found cyano-substituted oligo(*p*-phenylene vinylene) derivatives could change their emission colors under stretching when they were blended in linear low-density polyethylene.[14] We have reported that the emission of the benzoxazole derivatives bearing non-planar triphenylamine or phenothiazine moiety could be tuned by grinding.[15] Fraser et al have synthesized a series of β-diketone boron complexes with MFC behaviors.[16] As an analogue of β-diketone boron complexes, β-iminoenolate boron complexes often show strong emission in solutions and solid states. To the best of our knowledge, the MFC property of β-iminoenolate boron complex has not been reported. Therefore, we designed new carbazole and *tert*-butylcarbazole functionalized β-iminoenolate boron complexes **CB** and **TCB**, and the design strategies involved the following points. Firstly, D-π-A type conjugated compounds usually showed strong ICT emission, so carbazole unit was introduced due to the strong electron donating ability and strong luminance.[17] Secondly, in the reported β-iminoenolate boron complexes, the nitrogen-based ligands included quinolone, pyrimidine and pyrazine.[18] However, as an electron-deficiency unit, pyridine was not used as a ligand in β-iminoenolate boron complex. We deemed that the introduction of pyridine would increase the electron withdrawing ability of β-iminoenolate boron unit, favoring for ICT emission. Thirdly, we have previously found that *tert*-butyl can tune the self-assembling properties of carbazoles via enlarging the distance

between carbazole rings, leading to loose molecular packing in organogels,[19] which has been proved of importance in MFC properties. Herein, we found that the UV-vis absorption and fluorescent emission spectra of the two complexes in solutions were similar besides small red-shift of **TCB** compared with **CB** due to the electron-donating of *tert*-butyl groups. However, their solid emission behaviors were quite different. The as-synthesized crystal **CB** and **TCB** emitted orange and blue light under UV irradiation, respectively. After grinding the as-synthesized crystal **CB** for a while, it changed into yellow emitting powder and further into green-emitting powder after grinding with stronger force. In the case of **TCB**, it emitted bright green light after grinding. The fluorescent decay curves of **CB** revealed that the excimers were formed in the as-synthesized crystal, so the emitting color of **CB** was quite different from that of **TCB**, which could not form excimers in the as-synthesized crystal due to the steric hindrance of *tert*-butyl. Additionally, the emission changes of **CB** and **TCB** in different solid states were reversible upon treated by repeating mechanic grinding and fuming with CH_2Cl_2 (or heating). Therefore, the obtained β-iminoenolate boron complexes might be used as sensors and memory chips on the basis of the solid fluorescence response to external mechanical force and organic solvent.

Experimental Section

Measurement and characterization: ^{1}H and ^{13}C NMR spectra were measured with a Mercury Plus instrument at 400 MHz and 100 MHz by using DMSO-d_6 as the solvent in all cases. IR spectra were measured with a Nicolet-360 FT-IR spectrometer by incorporation of samples in KBr disks. The UV-vis absorption spectra were obtained on Shimadzu UV-3100 spectrophotometer. Fluorescent emission spectra were obtained on a Cary Eclipse fluorescence spectrophotometer. Cyclic voltammetry (CV) spectra of **CB** and **TCB** were obtained on a CHI 604C voltammetric analyzer with a scan rate at 50 mV/s. A three electrode configuration was used for the measurement: a platinum button as the working electrode, a platinum wire as the counter electrode, and a saturated calomel electrode (SCE) as the reference electrode. The solution of $(C_4H_9)_4NBF_4$ in CH_2Cl_2 (0.1M) was used as the supporting electrolyte. Mass spectra were obtained with Agilent 1100 MS series and AXIMA CFR MALDI-TOF (Compact) mass spectrometers. C, H, and N elemental analyses were performed with a Perkin–Elmer 240C elemental analyzer. XRD patterns were obtained on an Empyrean X-ray diffraction instrument. Single crystal of **CB** was selected for X-ray diffraction studies in a Rigaku RAXIS-RAPID diffractometer. Fluorescence lifetimes were obtained on a Edinburgh Instrument FLS920 fluorescence spectrophotometer, and all the samples were excited at 400 nm. The ground powder was prepared by grinding samples with a pestle in the morta. Ground powder 1 of **CB** was obtained by grinding the as-synthesized crystal of **CB** for 30 s. Ground powder 2 of **CB** was obtained by grinding ground powder 1 for another 5 min. Ground powder of **TCB** was obtained by grinding the as-synthesized crystal of **TCB** for 30 s.

Synthesis: THF was dried over sodium and diphenyl ketone. CH_2Cl_2 was dried over calcium hydride. The other chemicals and reagents were used as received without further purification. The synthetic routes for β-iminoenolate boron complexes **CB** and **TCB** were shown in Scheme 1. Firstly, the esters of methyl 4-(9H-carbazol-9-yl)benzoate **1**[20] and methyl 4-(3,6-di-tert-butyl-9H-carbazol-9-yl)benzoate **2**[19a] were synthesized according to the reported procedures. Then, the condensation coupling reactions between 2-methylpyridine and esters **1-2**, respectively, afforded the corresponding β-iminoenolate intermediates, which were complexed with boron trifluoride diethyl ether directly without further purification to yield the β-iminoenolate boron complexes **CB** and **TCB**. The target molecules were characterized by ^{1}H NMR, ^{13}C NMR, MALDI-TOF mass spectrometry, FT-IR and C, H, N elemental analyses (see Supporting Information). It was found that the synthesized β-iminoenolate boron complexes were dissolved in CH_2Cl_2, THF, and so on.

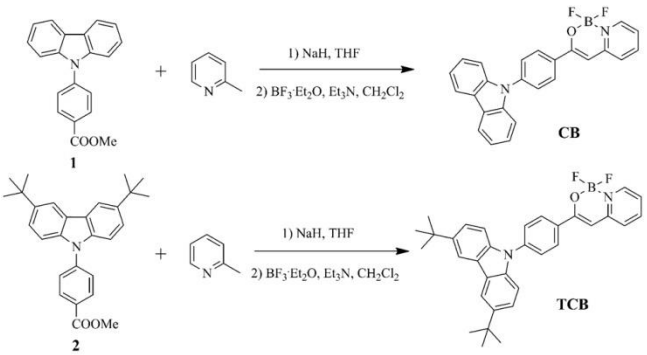

Scheme 1. Synthetic routes for β-iminoenolate boron complexes **CB** and **TCB**.

3-(4-(9H-carbazol-9-yl)phenyl)-1,1-difluoro-1H-pyrido[1,2-c][1,3,2]oxazaborinin-9-ium-1-uide (CB): NaH (60 %, 0.60 g, 15.14 mmol) was added to a solution of 2-methylpyridine (1.10 mL, 12.62 mmol) in THF (50mL) at 0 °C. Then, compound 1 (1.90 g, 6.31 mmol) was added and the mixture was stirred at room temperature for 30 min. After the mixture was refluxed under an atmosphere of nitrogen for 24 h, it was cooled to room temperature. After that, the mixture was acidified with dilute HCl and a yellow solid was collected by suction filtration. Then, the solid was dried under vacuum followed by dissolved in CH_2Cl_2 (50 mL). Boron trifluoride diethyl ether complex (4.00 mL, 31.55 mmol) and triethylamine (4.40 mL, 31.55 mmol) were added to the above solution, which was stirred at room temperature for 24 h. Water was added (200 mL) in order to quench the reaction. The organic layer was separated and dried over Na_2SO_4. After removal of the solvent, the crude product was purified by column chromatography (silica gel, petroleum ether/ethyl acetate, v/v = 3/1) to afford **CB** (0.96 g) as an orange solid. Yield 39%; m.p. 264.0-266.0 °C; ^{1}H NMR (400 MHz, DMSO-d_6) δ 8.60 (d, J = 4.0 Hz, 1H), 8.27 (t, J = 7.0 Hz, 6.0 Hz, 4H), 8.23 (s, 1H) 7.81 (d, J = 8.0 Hz, 2H), 7.74 (d, J = 8.0 Hz, 1H), 7.62 (t, J = 7.0 Hz, 6.0 Hz, 1H), 7.49 (m, 4H), 7.33 (t, J = 8.0 Hz, 8.0 Hz, 2H), 7.08 (s, 1H) (Figure S13); ^{13}C NMR (100 MHz, DMSO-d_6) δ 159.73, 150.97, 143.49, 140.40, 140.19, 139.49, 133.00, 128.25, 127.05, 126.88, 123.71, 123.50, 122.51, 121.08, 120.92, 110.28, 94.70 (Figure S14); IR (KBr): ν = 724, 754, 805, 910, 917, 1029, 1099, 1128, 1168, 1230, 1450, 1491, 1512, 1544, 1605, 1629, 2365, 2850, 2922 cm^{-1}; MALDI-TOF MS: m/z: calculated for $C_{25}H_{17}BF_2N_2O$: 410.14; found: 408.8 (Figure S15); elemental analysis (%) calculated for $C_{25}H_{17}BF_2N_2O$: C 73.20, H 4.18 , N 6.83; found: C 73.36, H 4.21, N 6.86.

3-(4-(3,6-di-tert-butyl-9H-carbazol-9-yl)phenyl)-1,1-difluoro-1H-pyrido[1,2-c][1,3,2]oxazaborinin-9-ium-1-uide (TCB): By following the synthetic procedure for **CB**, the intermediate was synthesized by compound 2 (1.50 g, 3.51 mmol) and 2-methylpyridine (0.69 mL, 7.02 mmol) in THF. Then the intermediate was reacted with boron trifluoride diethyl ether complex (2.20 mL, 17.55 mmol) in the presence of triethylamine (2.45 mL, 17.55 mmol) in CH_2Cl_2. The crude product was purified by column chromatography (silica gel; CH_2Cl_2) to afford **TCB** (0.51 g) as a light yellowish green solid. Yield 31%; m.p. 280.0-282.0 °C; ^{1}H NMR (400 MHz, DMSO-d_6) δ 8.57 (s, 1H), 8.32 (d, J = 1.6 Hz, 2H), 8.28 (m, 1H), 8.22 (d, J = 8.0 Hz, 2H), 7.80 (d, J = 8.0 Hz, 2H), 7.73 (d, J = 8.0 Hz, 1H), 7.61 (m, 1H), 7.52 (m, 2H), 7.44 (d, J = 9.0 Hz, 2H), 7.06 (s, 1H), 1.44 (s, 18H) (Figure S16); ^{13}C NMR (100 MHz, DMSO-d_6) δ 159.83, 151.02, 143.43, 140.36, 140.04, 138.52, 132.42, 128.18, 126.48, 124.33,123.67, 122.41, 117.25, 109.73, 94.52, 34.99 32.26 (Figure S17); IR (KBr): ν = 758, 801, 912, 1030, 1263, 1366, 1470, 1516, 1550, 1604, 1631, 2362, 2863, 2955 cm^{-1}; MALDI-TOF MS: m/z: calculated for $C_{33}H_{33}BF_2N_2O$: 522.3; found: 523.6 (Figure S18); elemental analysis (%) calculated for $C_{33}H_{33}BF_2N_2O$: C 75.87, H 6.37, N 5.36; found: C 76.10, H 6.40, N 5.39.

Results and discussion

UV-vis Absorption and Fluorescent Emission Spectra in Solutions

The UV-vis absorption and fluorescent emission spectra of **CB** and **TCB** in different solvents were shown in Figure 1, and the corresponding photophysical data were summarized in Table S1. It was clear that each β-iminoenolate boron complexe gave two strong absorption bands at ca. 292 nm and ca. 390 nm in solutions (Figure 1a and 1c). The absorption at ca. 292 nm coming from π-π* transition did not shift with increasing the polarity of the solvents, but the absorption at ca. 390 nm attributed to charge transfer (CT) transition, which was confirmed by solvent-dependent fluorescent emission spectral changes, blue-shifted with increasing solvent polarity. For example, the CT bands of **CB** and **TCB** emerge at 392 nm and 401 nm in cyclohexane, and blue-shifted to 381 nm and 391 nm in DMSO, respectively, which might be due to the less conjugation degree of β-iminoenolate boron complexes resulted from larger dihedral angle in more polar solvents.[15a] It should be noted that in the same solvent a red-shift of the absorption band of **TCB** compared with **CB** was detected (Table S1) on account of the introduction of electronic donating group of *tert*-butyls to carbazole unit in **TCB**. As shown in Figure 1c and 1d, in cyclohexane the emission bands of **CB** were located at 426 nm and 450 nm, and **TCB** gave two emission bands at 434 nm and 460 nm. The red-shift of the emission for **TCB** compared with **CB** was also ascribed to the weak electron donating ability of *tert*-butyl. Moreover, the emission bands for **CB** and **TCB** red-shifted obviously with increasing the solvent polarities. For example, **CB** emitted blue light centered at 458 nm in THF and green light located at 496 nm in DMSO (Figure 1b and Figure S1). Combined with the large Stokes shifts (2036-6085 cm^{-1}), the broadening and red-shift of the emission bands, we suggested that intramolecular charge transfer (ICT) transitions for **CB** took place in more polar solvents. It should be noted that **CB** gave two isolated emission peaks in non-polar solvents (cyclohexane and toluene), indicating that two separated close-lying excited states existed. We deduced that the emission of **CB** in cyclohexane and toluene was from the locally excited (LE) state.[21] Similarly, the emission of **TCB** in cyclohexane came from LE state, and the emissions in other solvents, including toluene, THF, CH_2Cl_2 and DMSO, were due to ICT transition. Because the molecular polarities of the synthesized β-iminoenolate boron complexes were in the order of **CB** < **TCB**, we could find that the ICT emission band of **TCB** appeared at lower energy region than that of **CB**. For instance, **TCB** emitted cyanine light (478 nm) in THF and yellow light (533 nm) in DMSO (Figure 1d and Figure S2). The

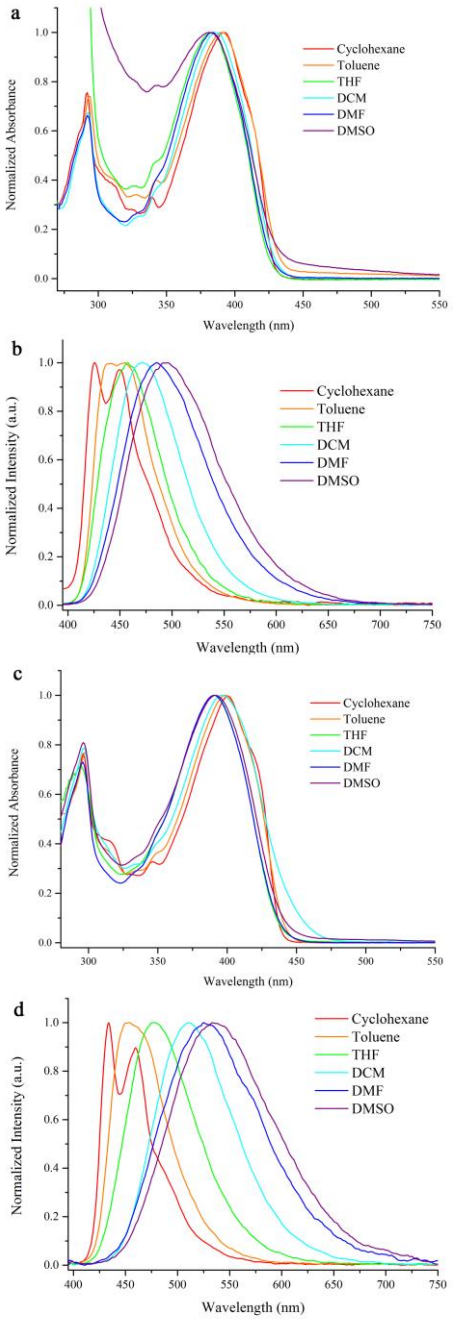

Figure 1. UV-vis absorption spectra of **CB** (a) and **TCB** (c), and fluorescent emission spectra of **CB** (b) and **TCB** (d) excited at 384 nm in different solvents (1 × 10^{-5} mol/L).

fluorescence quantum yields (Φ_F) of **CB** and **TCB** were measured using 9,10-diphenylanthracene in benzene (Φ_F = 0.85) as standard. The Φ_F for **CB** exhibited negative solvatokinetic effect[22] besides in DMSO, for example, it was only 0.16 in cyclohexane and increased with the increasing of the solvent polarity. The Φ_F of **CB** reached 0.67 in DMF. As to the Φ_F of **TCB**, negative solvatokinetic effect was also found in the solvents of cyclohexane, toluene, THF, CH_2Cl_2. The Φ_F of **TCB** reached the maximum of 0.65 in CH_2Cl_2, but decreased to 0.25 and 0.15 in DMF and DMSO (positive solvatokinetic effect in DMF and DMSO), respectively. The positive and negative solvatokinetic effects have also been found in stilbenoid derivatives and other ICT compounds with n-π^* and π-π^* electronic configurations.[23] In general, when energy level of excited state in polar solvent reduced due to the solvation effect, the energy gap would reduce and non-radiative transition would increase. Thus, the fluorescent quantum yield decreased in polar solvent, which was called positive solvatokinetic effect. On the other hand, when the compound with n electron was excited, several excited energy states existed and the proximity effect of n-π^* and π-π^* would cause energy loss and reduced the quantum yield. Therefore, the separation of the energy levels of n-π^* and π-π^* as well as the weakened proximity effect in polar solvents led to the negative slvatokinetic effect of Φ_F for **CB** and **TCB** in some polar solvents.

Electrochemical Properties

As shown in Figure S3, it was clear that **CB** and **TCB** exhibited two reversible reduction processes, and the half-wave potentials of **CB** were located at −2.17 V and −2.34 V (vs Fc/Fc^+), while those of **TCB** were located at −2.19 V and −2.37 V (vs Fc/Fc^+), respectively (Table 1). The reason that the reductive half-wave potential of **TCB** was lower than **CB** was due to the stronger electron donating ability of *tert*-butyl carbazole than carbazole. Additionally, the HOMO and LUMO energy levels were calculated using the empirical equations: $E_{LUMO} = -(E^{red} + 4.8)$ and $E_{HOMO} = E_{LUMO} - E_g$, in which E_g was estimated from the onset of the absorption spectrum ($E_g = 1240 / \lambda_{onset}$). It was found that the HOMO energy levels of **CB** and **TCB** were -5.53 eV and -5.38 eV, and the LUMO energy levels were -2.63 eV and -2.61 eV, respectively (Table 1).

Table 1. Electrochemical data and HOMO/LUMO energy levels of **CB** and **TCB**.

	E^{red} (V)[a]	LUMO (eV)[b]	HOMO (eV)[b]	E_g (eV)[c]	LUMO (eV)[d]	HOMO (eV)[d]
CB	-2.17, -2.34	-2.63	-5.53	2.90	-2.42	-5.57
TCB	-2.19, -2.37	-2.61	-5.38	2.77	-2.30	-5.31

[a] E^{red} = reduction potential; Fc/Fc^+ was used as external reference.

[b] Calculated using the empirical equation: $E_{LUMO} = -(E^{red} + 4.8)$ and $E_{HOMO} = E_{LUMO} - E_g$.

[c] Estimated from the onset of the absorption spectra ($E_g = 1240 / \lambda_{onset}$).

[d] Obtained from quantum chemical calculation using TDDFT/B3LYP/6-31G.

Theoretical Calculation

We carried out the density functional theory (DFT) calculations for β-iminoenolate boron complexes by Gaussian 09W program[24] using DFT/B3LYP/6-31G method to reveal the electronic structures of **CB** and **TCB**. The frontier orbital plots of the HOMO and LUMO were shown in Figure 2. We could find that the LUMO was mainly distributed in the acceptor of β-iminoenolate boron unit for **CB** and **TCB**, and the HOMO of **CB** was located in the whole molecule. With increasing the polarity of **TCB**, the HOMO of **TCB** was mainly located in *tert*-butyl carbazole unit. As a result, the intramolecular charge transfer would occur in the D-π-A type β-iminoenolate boron complexes. Moreover, the calculated energy levels of HOMO and LUMO for **CB** and **TCB** were close to those based on CV results (Table 1).

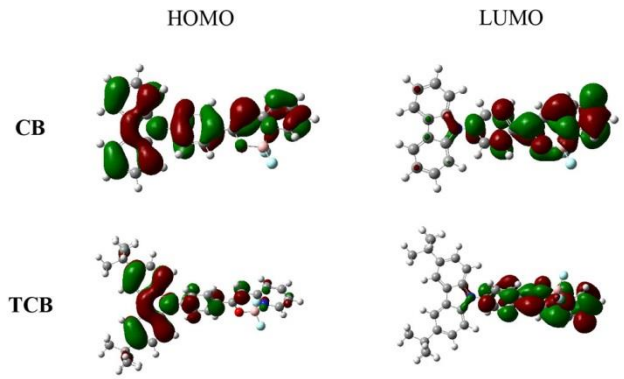

Figure 2. The frontier orbital plots of the HOMO and LUMO of **CB** and **TCB**.

Mechanofluorochromic Properties

As discussed above, the synthesized β-iminoenolate boron complexes exhibited similar fluorescent emission properties in solutions. However, from Figure 3 we could find that the emitting colors of **CB** and **TCB** either in as-synthesized crystal or in ground powders, which were obtained by means of mechanic grinding, were quite different under UV illumination. Meanwhile, the emission switch could be achieved by repeating treatment of mechanic grinding/fuming with CH_2Cl_2 or heating. In order to study such morphology-dependent and molecular structure-dependent solid emission properties, the fluorescent emission spectra of **CB** and **TCB** in different solid states were given in Figure 4 and Figure 7. Upon illuminated by the light of 365 nm, the as-synthesized crystal of **CB** emitted orange light with two emission bands at 465 nm and 553 nm, and the emission intensity at 553 nm was ca. twice as high as that at 465 nm. After ground for a while, the crystal turned into ground powder 1 with bright yellow emission, and the emission bands were located at 465 nm and 550 nm. Although the emission peaks of **CB** in ground powder 1 did not shift obviously compared with the as-synthesized crystal, the ratio of the emission intensities at 465 nm and 550 nm turned to ca. 1/1. Further grinding the ground power 1 of **CB**, only one broad emission band centered at 487 nm appeared in the ground powder 2, emitting dark green light. It should be noted that the emission of the ground powder 2 of **CB** could be split into two bands at 460 nm and 545 nm after fumed with CH_2Cl_2 for 5 s or heated for a certain time, and we signed it as the fumed sample. We found that the higher was the heating temperature, the shorter was the recovery time. It would take 2 min for the recovery from ground powder 2 to ground powder 1 at 80 °C,

and the recovery time could be shortened to 20 s and 10 s at 100 °C and 120 °C, which were much lower than its melting point (264.0-266.0 °C), respectively. Although the emission intensity at 460 nm was not same as that at 545 nm (in a ratio of 3/2), the fumed sample of **CB** still emitted bright yellow light, which was similar to ground powder 1. Thus, the fumed sample was regarded as ground powder 1. The transformation between ground powder 1 and 2 was reversible under grinding/heating or fuming treatment (Figure S4). In addition, the fluorescence quantum yield of **CB** in ground powder 2 increased to 0.25 from 0.19 in as-synthesized crystal.

Figure 3. Photos of **CB** and **TCB** in different solid states under UV light (365 nm).

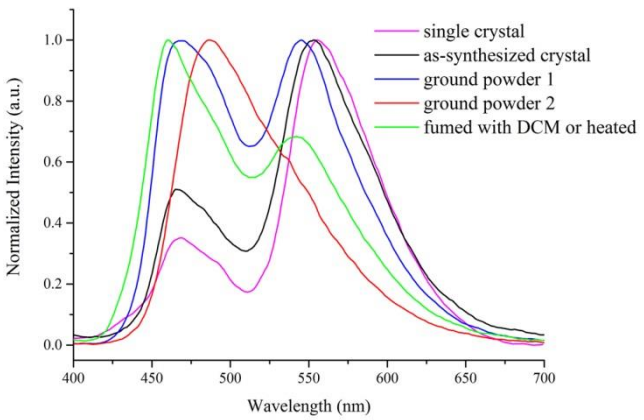

Figure 4. Fluorescence emission spectra of **CB** in different solid states (λ_{ex} = 365 nm).

To verify the MFC phenomenon was induced by the morphology, XRD patterns of **CB** in different solid states were shown in Figure 5. The as-synthesized crystal gave sharp and strong peaks because of the ordered organization of **CB** molecules. When the as-synthesized crystal was ground to powder 1, the diffraction peaks were still sharp and strong, suggesting some crystal structures were maintained. After further ground, the diffraction peaks of the ground powder 2 became very weak, meaning the amorphous state. Upon fuming with CH_2Cl_2 or heating ground powder 2, the diffraction peaks recovered, illustrating that certain amount of the crystalline structures reformed. Thus, the solid fluorescence switch of **CB** could be achieved via grinding/fuming (or heating) treatment, and the different emitting colors of **CB** in solid states resulted from the transformation between crystalline and amorphous states.

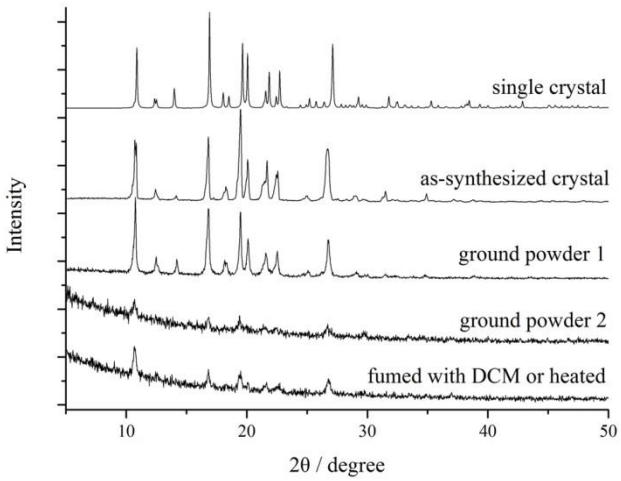

Figure 5. XRD patterns of **CB** in different solid states.

Furthermore, the single crystal of **CB** was obtained by evaporation of the solution in dichloromethane/methanol to reveal the molecular packing mode in crystals, which would affect its emission. We found that the XRD pattern and fluorescent emission spectrum of **CB** in single crystal were similar to those in as-synthesized crystal (Figure 4 and 5), and deduced that similar molecule stacking modes might be involved in the as-synthesized crystal and in single crystal. As shown in Figure 6, we could find that the interactions between pyridine and the benzene connected to carbazole happened, and the distances of C(Ar)•••C(Ar) were 3.32 Å and 3.50 Å (Figure 6c), corresponding to the distance of π-π interaction. Moreover, the hydrogen bonds of C(Ar)-H•••F, C(Ar)-H•••O and C(Ar)-H•••B were formed in the single crystal. In detail, one of the fluorine atoms in the central molecule formed hydrogen bond with the hydrogen atom in the pyridine ring of the adjacent molecule (2.51 Å), and the other fluorine atom interacted with the hydrogen atom on the 4-position of carbazole in the other adjacent molecule via hydrogen bond (2.52 Å). In addition, the 4-position hydrogen atom of carbazole formed hydrogen bond with the boron and nitrogen atoms in the central molecule with distances of 3.05 Å and 2.70 Å, respectively. Based on the single crystal structure of **CB**, we deduced that the emission band at 533 nm in as-synthesized crystal came from the excimers, and the one located at 465 nm might be due to the electronic transition of the isolated molecules, which could be confirmed by their fluorescence lifetimes. The luminescence decay curve of **CB** in the as-synthesized crystal monitored at 465 nm gave an average lifetime of 0.81 ns (Figure S5), which was similar to the fluorescence lifetime of 0.75 ns for the emission at 470 nm in dilute toluene (Figure S6). Therefore, we deemed the emission at 465 nm from the monomers. However, the average lifetime for the emission peak at 553 nm was much longer than that at 465 nm, and reached 16.11 ns (Figure S7), and we ascribed it as the emission of the excimers. When ground into powder 1, the as-synthesized crystal of **CB** turned into small crystals and certain amount of monomers disappeared. Thus, the emission intensity at 553 nm due to the excimers decreased and the emission at 465 nm from monomers increased. After further ground, the crystalline structure was almost damaged and no emission from the excimers could be detected, so only one broad emission band

centered at 487 nm emerged in the amorphous ground powder 2. Moreover, upon fuming with CH_2Cl_2 or heating the ground powder 2, the sample gave two isolated emission bands (465 nm and 545 nm), meaning new excimers were formed again. The reason why the ratio of the emission intensities at ca. 460 nm and ca. 550 nm in the fumed sample was higher than that in the as-synthesized crystal was that the amount of the excimers in the fumed sample was less than that in the as-synthesized crystal. Therefore, the β-iminoenolate boron complexes with varied solid emissions tuned by mechanical force stimuli and organic solvent fuming may be employed in sensors and memory chips.

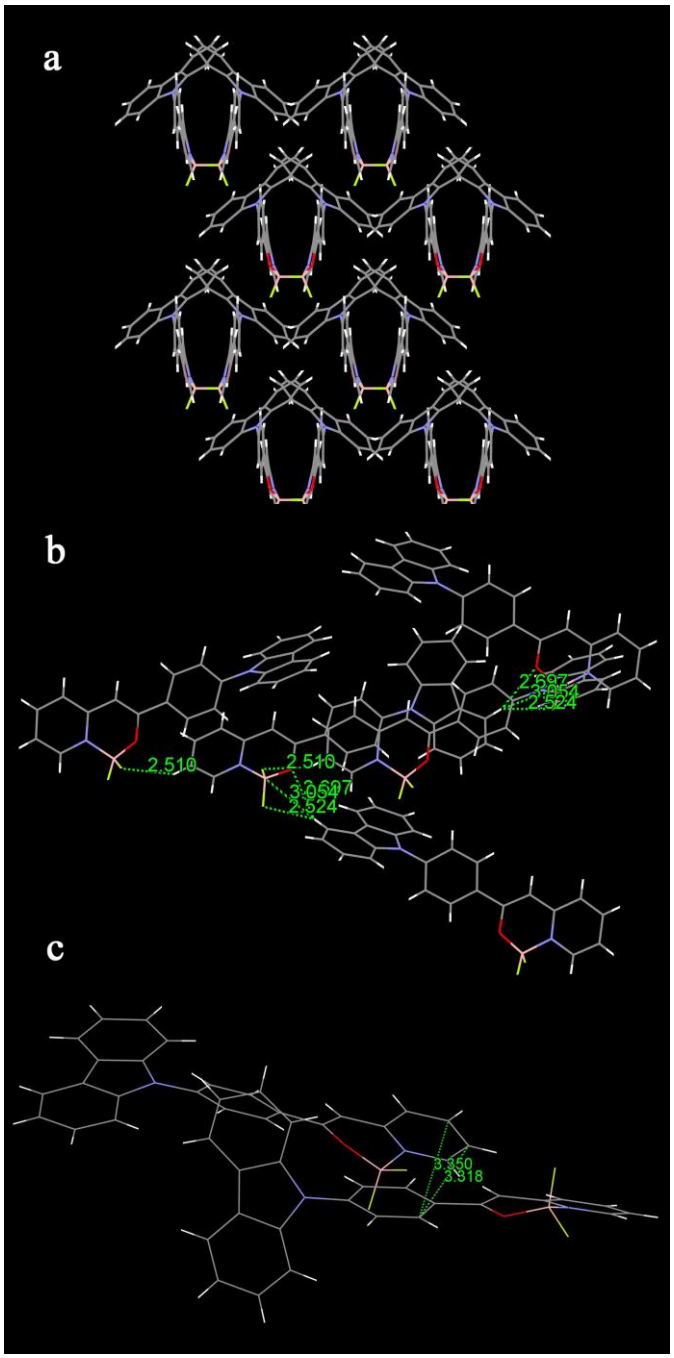

Figure 6. Single crystal structure of **CB**. a) side view, b) hydrogen bonds between the molecules and c) π-π interactions in crystal.

It was interesting that **TCB** showed totally different MFC properties from **CB**. As shown in Figures 3 and 7, **TCB** emitted blue light centered at 462 nm in the as-synthesized crystal and emitted bright green light located at 501 nm in ground powder upon excited at 365 nm. The ground powder gave an emission at 501 nm with Φ_F of 0.53, which was higher than that in the as-synthesized crystal (0.29). Notably, the Φ_F of the obtained ground powder **TCB** was the highest one for the β-iminoenolate boron complexes that have ever been reported. When the ground powder was fumed with CH_2Cl_2 for 5 s, the emission returned to 463 nm, similar to the as-synthesized crystal. Additionally, heating also could make the emission of the ground powder recover to 463 nm. It took 10 min to recover at 135 °C, and only 60 s, 30 s and 10 s were needed for the recovery at 145 °C, 160 °C and 190 °C, which were lower than the melting point (280.0-282.0 °C), respectively. The transformation between the as-synthesized crystal and the ground powder of **TCB** was also reversible under grinding and heating/fuming treatment (Figure S8). To reveal the relationship between the morphologies and the solid emission behaviors, the XRD patterns of **TCB** in different solid states were shown in Figure 8. The as-synthesized crystal gave several sharp and strong peaks, which disappeared in the ground powder, meaning that the crystal was damaged intoamorphous state. After fumed with CH_2Cl_2 or heated, the amorphous state converted to crystalline state in accordance with the recovery of diffraction peaks. We also intended to gain the single crystal of **TCB**, but failed.

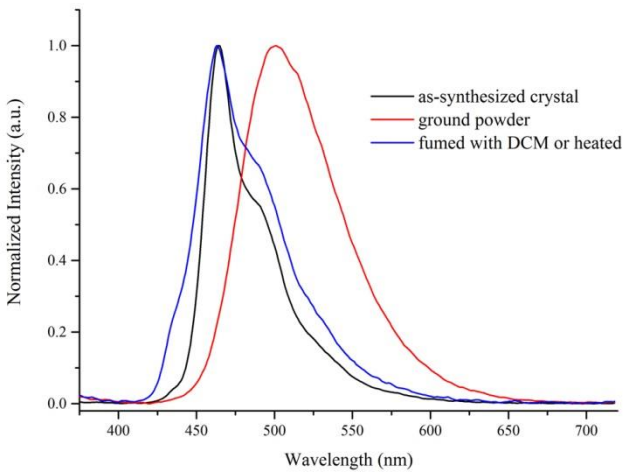

Figure 7. Fluorescence emission spectra of **TCB** in different solid states (λ_{ex} = 365 nm).

To explain the different MFC behavior of **TCB** compared with **CB**, the fluorescence decay curves of **TCB** in toluene and in different solid states were shown in Figure S9-12. We found that the average fluorescence lifetime of the emission at 462 nm for **TCB** in as-synthesized crystal was 1.89 ns, which was similar to that of the emission at 454 nm in dilute toluene (1.65 ns). Therefore, we deduced that the emission of **TCB** in as-synthesized crystal was coming from the monomers. Moreover, the lifetime of emission at ca. 480 nm (shoulder) in as-synthesized crystal was 1.99 ns, closing to that at 462 nm. It further illustrated that **TCB** existed as monomers in as-synthesized crystal. However, the lifetime of the emission at 501 nm for **TCB** in the ground powder increased to 5.28 ns, suggesting the formation of excimer. In our previous work, we

have found that *tert*-butyl could enlarge the distance between the adjacent carbazole molecules in the aggregated state.[19] In the case of **TCB**, the introduction of *tert*-butyl would prevent the formation the excimers in the crystalline state due to the steric hindrance. After ground, the molecules might stack together to some extent, and the excimer could be formed, as a result, the fluorescence quantum yield of **TCB** increased significantly (0.53) in ground powder compared with that in as-synthesized crystal.

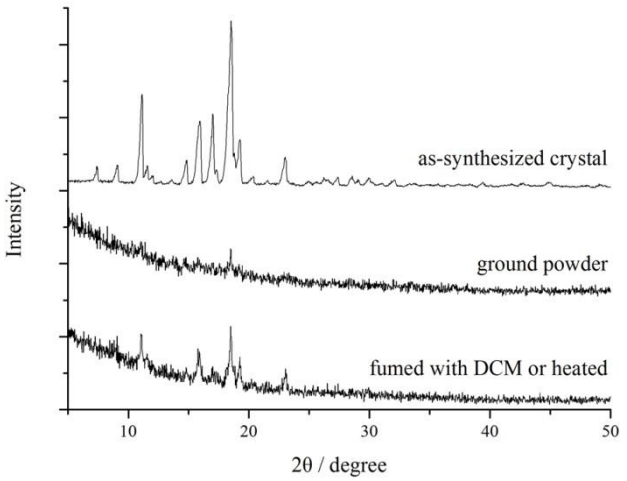

Figure 8. XRD patterns of **TCB** in different solid states.

Conclusions

In summary, we synthesized carbazole and *tert*-butylcarbazole functionalized β-iminoenolate boron complexes **CB** and **TCB**. It was found that they exhibited strong emission in solutions, and the Φ_F of **CB** and **TCB** in CH_2Cl_2 were 0.58 and 0.65, respectively, using 9,10-diphenylanthracene in benzene as standard. Notably, their solid emissions were dependent not only on the morphologies but also on the molecular structures. For instance, the as-synthesized crystal of **CB** emitted orange light with two emission bands at 465 nm and 553 nm under UV irradiation. The fluorescent decay curves illustrated that the emission at 465 nm came from the monomers, and the emission at 553 nm was due to the formed excimers. After grinding the as-synthesized crystal for a while, the ground powder 1 composed of small crystals and certain amount of monomers emitted bright yellow light since the emission intensity of excimers decreased and emission of monomers increased. Further grinding for a long time, the obtained amorphous ground powder 2 of **CB** emitted dark green light on account of the disappearance of the excimers. It was interesting that **TCB** emitted sky blue light centered at 462 nm under UV irradiation in as-synthesized crystal because no excimers were formed due to the steric hindrance of *tert*-butyl. After grinding, the amorphous ground powder of **TCB** emitted bright green light derived from excimers. Notably, the fluorescent quantum yield of **TCB** in amorphous solid state reached 0.53, which was the highest one for the β-iminoenolate boron complexes that have ever been reported. Herein, we provided a strategy to design new boron complexes with high solid emission via restraining the formation of the aggregates by introduction of bulky groups. Additionally, the emission changes of **CB** and **TCB** in different solid states were reversible upon treated by repeating mechanic grinding and fuming (or heating), so that such solid fluorescence response to external mechanical force and organic solvent made β-iminoenolate boron complexes be potentially applied in sensors and memory chips.

Acknowledgements

This work is financially supported by the National Natural Science Foundation of China (21374041), the Open Project of State Key Laboratory of Supramolecular Structure and Materials (SKLSSM201407) and the Open Project of State Key Laboratory of Theoretical and Computational Chemistry (K2013-02).

Notes and references

[a] State Key Laboratory of Supramolecular Structure and Materials, College of Chemistry, Jilin University, Changchun, P.R. China. E-mail: luran@mail.jlu.edu.cn

[b] State Key Laboratory of Theoretical and Computational Chemistry, Institute of Theoretical Chemistry, Jilin University, Changchun, P.R. China.

†

Electronic Supplementary Information (ESI) available: [^{1}H NMR, ^{13}C NMR, MALDI/TOF MS and CV spectra of target molecules; photophysical data, photos in solutions under UV light and the emission changes upon ground and fumed with CH_2Cl_2 for target compounds; time-resolved emission-decay curve of compound CB. Deposition numbers of the single crystal of compound CB is CCDC 1010373]. See DOI: 10.1039/b000000x/

1 a) A. C. Grimsdale, K. L. Chan, R. E. Martin, P. G. Jokisz, A. B. Holmes, *Chem. Rev*., 2009, **109**, 897-1091; b) S. M. Kelly, *Flat Panel Displays: Advanced Organic Materials* (Ed.: J. A. Connor), The Royal Society of Chemistry, Cambridge, 2000.

2 F. Cicoira, C. Santato, *Adv. Funct. Mater*., 2007, **17**, 3421-3434.

3 a) I. D. W. Samuel, G. A. Turnbull, *Chem. Rev*. 2007, **107**, 1272-1295; b) U. Scherf, S. Riechel, U. Lemmer, R. F. Mahrt, Curr. Opin. Solid State *Mater. Sci*., 2001, **5**, 143-154; c) M. D. McGehee, A. J. Heeger, *Adv. Mater*., 2000, **12**, 1655; d) G. Kranzelbinder, G. Leising, *Rep. Prog. Phys*., 2000, **63**, 729-762; e) N. Tessler, *Adv. Mater*., 1999, **11**, 363-370; f) V. G. Kozlov, S. R. Forrest, *Curr. Opin. Solid State Mater. Sci*., 1999, **4**, 203-208.

4 a) S. Sreejith, K. P. Divya, A. Ajayaghosh, *Chem. Commun*., 2008, 2903-2905; b) T. J. Dale, J. Rebek, *J. Am. Chem. Soc*., 2006, **128**, 4500-4501; c) S. W. Zhang, T. M. Swager, *J. Am. Chem. Soc*., 2003, **125**, 3420-3421; d) J. S. Yang, T. M. Swager, *J. Am. Chem. Soc*., 1998, **120**, 11864-11873; k) J. S. Yang, T. M. Swager, *J. Am. Chem. Soc*., 1998, **120**, 5321-5322.

5 a) Z. G. Chi, X. Q. Zhang, B. J. Xu, X. Zhou, C. P. Ma, Y. Zhang, S. W. Liu and J. R. Xu, *Chem. Soc. Rev*., 2012, **41**, 3878-3896. b) X. Q. Zhang, Z. G. Chi, Y. Zhang, S. W. Liu and J. R. Xu, *J. Mater. Chem. C*, 2013, **1**, 3376-3390.

6 a) M. S. Kwon, J. Gierschner, J. Seo and S. Y. Park, *J. Mater. Chem. C*, 2014, **2**, 2552-2557; b) X. Cheng, D. Li, Z. Y. Zhang, H. Y. Zhang and Y. Wang, *Org. Lett*., 2014, **16**, 880-883; c) Y. J. Zhang, J. W. Sun, G. L. Zhuang, M. Ouyang, Z. W. Yu, F. Cao, G. X. Pan, P. S. Tang, C. Zhang and Y. G. Ma, *J. Mater. Chem. C*, 2014, **2**, 195-200.

7 a) A. Pucci, F. D. Cuia, F. Signoriab and G. Ruggeri, *J. Mater. Chem*., 2007, **17**, 783-790; b) M. Kinami, B. R. Crenshaw and C. Weder, *Chem. Mater*., 2006, **18**, 946-955.

8 a) S. Hirata, T. Watanabe, *Adv. Mater*., 2006, **18**, 2725-2729; b) S. J. Lim, B. K. An, S. D. Jung, M. A. Chung, S. Y. Park, *Angew. Chem, Int. Ed*., 2004, **43**, 6346-6350; c) M. Irie, T. Fukaminato, T. Sasaki, N. Tamai, T. Kawai, *Nature*, 2002, **420**, 759-760.

9 A. Kishimura, T. Yamashita, K. Yamaguchi, T. Aida, *Nat. Mater*., 2005, **4**, 546-549.

10 a) W. Z. Yuan, Y. G. Gong, S. M. Chen, X. Y. Shen, J. W. Y. Lam, P. Lu, Y. W. Lu, Z. M. Wang, R. R. Hu, N. Xie, H. S. Kwok, Y. M. Zhang, J. Z. Sun and B. Z. Tang, *Chem. Mater*., 2012, **24**, 1518-1528; b) Y. Y. Gong, Y. R. Zhang, W. Z. Yuan, J. Z. Sun, and Y. M. Zhang, *J. Phys. Chem. C*, 2014, **118**, 10998–11005; c) Y. Y. Gong, Y. Q. Tan, J. Liu, P. Lu, C. F. Feng, W. Z. Yuan, Y. W. Lu, J. Z. Sun, G. F. He and Y. M. Zhang, *Chem. Commun*., 2013, **49**, 4009-4011.

11 a) C. P. Ma, B. J. Xu, G. Y. Xie, J. J. He, X. Zhou, B. Y. Peng, L. Jiang, B. Xu, W. J. Tian, Z. G. Chi, S. W. Liu, Y. Zhang and J. R. Xu, *Chem. Commun*., 2014, **50**, 7374-7377; b) H. Li, Z. Chi, B. Xu, X. Zhang, X. Li, S. Liu, Y. Zhang and J. Xu, *J. Mater. Chem*., 2011, **21**, 3760-3767; c) Q. K. Qi, J. B. Zhang, B. Xu, B. Li, S. X. A. Zhang and W. J. Tian, *J. Phys. Chem. C*, 2013, **117**, 24997-25003; d) M. P. Aldred, G. F. Zhang, C. Li, G. Chen, T. Chen and M. Q. Zhu, *J. Mater. Chem. C*, 2013, **1**, 6709-6718; e) Y. Lu, Y. Tan, Y. Gong, H. Li, W. Yuan, Y. Zhang and B. Tang, *Chin. Sci. Bull*., 2013, **58**, 2719-2722.; f) W. Z. Yuan, Y. Q. Tan, Y. Y. Gong, P. Lu, J. W. Y. Lam, X. Y. Shen, C. F. Feng, H. H-Y. Sung, Y. W. Lu, I. D. Williams, J. Z. Sun, Y. M. Zhang and B. Z. Tang, *Adv. Mater*., 2013, **25**, 2837-2843.

12 a) X. Zhang, Z. Chi, J. Zhang, H. Li, B. Xu, X. Li, S. Liu, Y. Zhang and J. Xu, *J. Phys. Chem. B*, 2011, **115**, 7606-7611; b) H. Li, X. Zhang, Z. Chi, B. Xu, W. Zhou, S. Liu, Y. Zhang and J. Xu, *Org. Lett*., 2011, **13**, 556-559; c) Y. J. Dong, B. Xu, J. B. Zhang, X. Tan, L. J. Wang, J. L. Chen, H. G. Lv, S. P. Wen, B. Li, L. Ye, B. Zou, and W. J. Tian, *Angew. Chem. Int. Ed*., 2012, **51**, 10782-10785; d) Y. J. Dong, J. B. Zhang, X. Tan, L. J. Wang, J. L. Chen, B. Li, L. Ye, B. Xu, B. Zou and W. J. Tian, *J. Mater. Chem. C*, 2013, **1**, 7554-7559.

13 a) J. Kunzelman, M. Kinami, B. R. Crenshaw, J. D. Protasiewicz and C. Weder, *Adv. Mater*., 2008, **20**, 119-122; b) S. J. Yoon, J. W. Chung, J. Gierschner, K. S. Kim, M. G. Choi, D. Kim and S. Y. Park, *J. Am. Chem. Soc*., 2010, **132**, 13675-13683; c) S. J. Yoon and S. Y. Park, *J. Mater. Chem*., 2011, **21**, 8338-8346; d) J. W. Sun, X. J. Lv, P. J. Wang, Y. J. Zhang, Y. Y. Dai, Q. C. Wu, M. Ouyang and C. Zhang, *J. Mater. Chem. C*, 2014, **2**, 5365-5371.

14 C. Löwe and C. Weder, *Adv. Mater*., 2002, **14**, 1625-1629.

15 a) P. C. Xue, B. Q. Yao, J. B. Sun, Q. X. Xu, P. Chen, Z. Q. Zhang and R. Lu, *J. Mater. Chem. C*, 2014, **2**, 3942-3950; b) P. C. Xue, P. Chen, J. H. Jia, Q. X. Xu, J. B. Sun, B. Q. Yao, Z. Q. Zhang and R. Lu, *Chem. Commun*., 2014, **50**, 2569-2571.

16 a) G. Zhang, J. Lu, M. Sabat and C. L. Fraser, *J. Am. Chem. Soc*., 2010, **132**, 2160-2162; b) G. Zhang, J. P. Singer, S. E. Kooi, R. E. Evans, E. L. Thomas and C. L. Fraser, *J. Mater. Chem*., 2011, **21**, 8295-8299; c) N. D. Nguyen, G. Zhang, J. Lu, A. E. Sherman and C. L. Fraser, *J. Mater. Chem*., 2011, **21**, 8409-8415; d) G. Zhang, J. Lu and C. L. Fraser, *Inorg. Chem*., 2010, **49**, 10747-10749; e) T. Liu, A. D. Chien, J. Lu, G. Zhang and C. L. Fraser, *J. Mater. Chem*., 2011, **21**, 8401-8408; f) P. Galer, R. C. Korošec, M. Vidmar and B. Šket, *J. Am. Chem. Soc*., 2014, **136**, 7383–7394.

17 a) T. H. Xu, R. Lu, X. L. Liu, X. Q. Zheng, X. P. Qiu, Y. Y. Zhao, *Org. Lett*., 2007, **9**, 797-800; b) T. H. Xu, R. Lu, X. L. Liu, P. Chen, X. P. Qiu, Y. Y. Zhao, *Eur. J. Org. Chem*., 2008, 1065-1071; c) T. H. Xu, R. Lu, X. L. Liu, P. Chen, X. P. Qiu, Y. Y. Zhao, *J. Org. Chem*., 2008, **73**, 1809-1817; d) X. L. Liu, R. Lu, T. H. Xu, D. F. Xu, Y. Zhan, P. Chen, X. P. Qiu, Y. Y. Zhao, *Eur. J. Org. Chem*., 2009, 53-60; e) X. L. Liu, D. F. Xu, R. Lu, B. Li, C. Qian, P. C. Xue, X. F. Zhang, H. P. Zhou, *Eur. Chem. J*., 2011, **17**, 1660-1669; f) X. L. Liu, X. F. Zhang, R. Lu, P. C. Xue, D. F. Xu, H. P. Zhou, *J. Mater. Chem*., 2011, **21**, 8756-8765.

18 a) Y. Zhou, Y. Xiao, S. M. Chi, X. H. Qian, *Org. Lett*., 2008, **10**, 633-636; b) J. Q. Feng, B. L. Liang, D. L. Wang, L. Xue, X. Y. Li, *Org. Lett*., 2008, **10**, 4437-4440; c) Y. Kubota, Y. Ozaki, K. Funabiki, M. Matsui, *J. Org. Chem*., 2013, **78**, 7058-7067; d)Y. Kubota, H. Hara, S. Tanaka, K. Funabiki, Masaki Matsui, *Org. Lett*., 2011, **13**, 6544-6547.

19 a) X. C. Yang, R. Lu, F. Y. Gai, P. C. Xue, Y. Zhan, *Chem. Commun*., 2010, **46**, 1088-1090; b) X. C. Yang, R. Lu, T. H. Xu, P. C. Xue, X. L. Liu and Y. Y. Zhao, *Chem. Commun*., 2008, 453-455; c) D. F. Xu, X. L. Liu, R. Lu, P. C. Xue, X. F. Zhang, H. P. Zhou and J. H. Jia, *Org. Biomol. Chem*., 2011, **9**, 1523-1528.

20 J. H. Cho, Y. S. Ryu, S. H. Oh, J. K. Kwon, E. K. Yum, *Bull. Korean Chem. Soc*., 2011, **32**, 2461-2464.

21 a) G. Jones II., W. R. Jackson, C. Choi, W. R. Bergmark, *J. Phys. Chem*., 1985, **89**, 294-300; b) S. Nad, H. Pal, *J. Phys. Chem. A*, 2001, **105**, 1097-1106; c) F. Loiseau, S. Campagna, A. Hameurlaine, W. Dehaen, *J. Am. Chem. Soc*., 2005, **127**, 11352-11363.

22 S. K. Wu, *Progress in Chemistry*, 2005, **17**, 15-39.

23 P. F. Wang, Z. Y. Xie, Z. R. Hong, J. X. Tang, O. Wong, C. S. Lee, N. Wong, S. Lee, *J. Mater. Chem*., 2003, **13**, 1894-1899.

24 M. J. Frisch, G. W. Trucks, H. B. Schlegel, G. E. Scuseria, M. A. Robb, J. R. Cheeseman, G. Scalmani, V. Barone, B. Mennucci, G. A. Petersson, H. Nakatsuji, M. Caricato, X. Li, H. P. Hratchian, A. F. Izmaylov, J. Bloino, G. Zheng, J. L. Sonnenberg, M. Hada, M. Ehara, K. Toyota, R. Fukuda, J. Hasegawa, M. Ishida, T. Nakajima, Y. Honda, O. Kitao, H. Nakai, T. Vreven, J. A. Montgomery, Jr, J. E. Peralta, F. Ogliaro, M. Bearpark, J. J. Heyd, E. Brothers, K. N. Kudin, V. N. Staroverov, R. Kobayashi, J. Normand, K. Raghavachari, A. Rendell, J. C. Burant, S. S. Iyengar, J. Tomasi, M. Cossi, N. Rega, J. M. Millam, M. Klene, J. E. Knox, J. B. Cross, V. Bakken, C. Adamo, J. Jaramillo, R. Gomperts, R. E. Stratmann, O. Yazyev, A. J. Austin, R. Cammi, C. Pomelli, J. W. Ochterski, R. L. Martin, K. Morokuma, V. G. Zakrzewski, G. A. Voth, P. Salvador, J. J. Dannenberg, S. Dapprich, A. D. Daniels, Ö. Farkas, J. B. Foresman, J. V. Ortiz, J. Cioslowski and D. J. Fox, *Gaussian 09, Revision A.02*, Gaussian, Inc., Wallingford, CT, 2009.

